IEEE Open Journal of Vehicular Technology

Received 18 October 2024; accepted 20 November 2024. Date of publication 25 November 2024;
date of current version 19 December 2024. The review of this article was coordinated by Editor Liwei Zhou.

Digital Object Identifier 10.1109/OJVT.2024.3505778

Harmonics Measurement, Analysis, and Impact Assessment of Electric Vehicle Smart Charging

MURAT SENOL [1] (Graduate Student Member, IEEE), I. SAFAK BAYRAM [1] (Senior Member, IEEE), LEWIS HUNTER [1] (Member, IEEE), KRISTIAN SEVDARI [2] (Member, IEEE), CONNOR MCGARRY [1] (Member, IEEE), DAVID CAMPOS GAONA [1] (Senior Member, IEEE), OLIVER GEHRKE [2] (Member, IEEE), AND STUART GALLOWAY [1] (Member, IEEE)

[1]Department of Electronic and Electrical Engineering, University of Strathclyde, G1 1XW Glasgow, U.K.
[2]Department of Wind and Energy Systems, Technical University of Denmark (DTU), 4000 Roskilde, Denmark

CORRESPONDING AUTHOR: MURAT SENOL (e-mail: murat.senol@strath.ac.uk).

This work was supported by EU H2020 Research Infrastructure Erigrid Project 2.0 under Grant 870620. The work of Murat Senol was supported by the Republic of Türkiye Ministry of National Education. The work of Kristian Sevdari was supported in part by AHEAD PROJECT Horizon Europe under Grant 101160665 and in part by EV4EU PROJECT Horizon Europe under Grant 101056765.

ABSTRACT Smart charging for Electric Vehicles (EVs) is gaining traction as a key solution to alleviate grid congestion, delay the need for costly network upgrades, and capitalize on off-peak electricity rates. Governments are now enforcing the inclusion of smart charging capabilities in EV charging stations to facilitate this transition. While much of the current research focuses on managing voltage profiles, there is a growing need to examine harmonic emissions in greater detail. This study presents comprehensive data on harmonic distortion during the smart charging of eight popular EV models. We conducted an experimental analysis, measuring harmonic levels with charging current increments of 1A, ranging from the minimum to the maximum for each vehicle. The analysis compared harmonic emissions from both single and multiple EV charging scenarios against the thresholds for total harmonic distortion (THD) and individual harmonic limits outlined in power quality standards (e.g. IEC). Monte Carlo simulations were employed to further understand the behavior in multi-vehicle scenarios. The results reveal that harmonic distortion increases as the charging current decreases across both single and multiple vehicle charging instances. In case studies where several vehicles charge simultaneously, the findings show that as more EVs charge together, harmonic cancellation effects become more pronounced, leading to a gradual reduction in overall harmonic distortion. However, under worst-case conditions, the aggregate current THD can rise as high as 25%, with half of the tested vehicles surpassing the individual harmonic limits.

INDEX TERMS Electric vehicles, harmonic distortion, smart charging, power grid impacts, power quality.

I. INTRODUCTION

A. MOTIVATION

Many governments worldwide have set ambitious goals to achieve climate neutrality within the next few decades [1], with the transportation sector coming under particular scrutiny due to its significant contribution to greenhouse gas emissions [2]. The transition to electric vehicles (EVs) is widely seen as a critical step in cutting emissions from road transport. This shift is further supported by reducing both the frequency and distance of trips, as well as encouraging the use of alternative low-carbon transportation options such as buses and trains [3]. However, the widespread adoption of EVs demands a seamless integration between aging power grids and expanding EV charging networks. As a result, the success of electrification hinges on several factors, including the rate of grid upgrades, the volume and distribution of EV sales, the development and timing of charging infrastructure, regulatory and policy decisions, and broader economic conditions [4].

Smart charging is increasingly seen as an effective solution to mitigate the negative impact of uncontrolled EV charging on electrical power systems [5], [6]. This approach leverages the natural flexibility of EV charging, which stems from the gap between the time a vehicle is parked and the actual duration required to charge it [7], [8], [9]. For instance, a typical domestic charging window might span from 7 pm to 7 am (12 hours), yet less than half of this period may be needed to charge 100 miles of electric range [10]. Smart charging is also used in parking lots with EV chargers to manage peak loads and reduce infrastructure costs [11]. In response to these benefits, the U.K. Government has introduced the Electric Vehicle Smart Charge Points Regulations, which require that EV charging stations incorporate smart functionality [12]. Smart charging during peak hours is also becoming common in the City of Amsterdam, where charging rates are limited between 6 pm and 9 pm to reduce the stress on the grid [13].

In addition to reducing peak EV demand and optimizing load profiles [14], smart charging frameworks are increasingly being discussed in both academia and industry. These frameworks are designed to mitigate voltage drops and reduce transformer stress, particularly for domestic charging [15], as well as balance phases in commercial applications [16]. Beyond the technical benefits for the grid, smart charging also offers financial advantages for consumers by shifting charging sessions to off-peak times when electricity rates are lower [17]. Despite these benefits, there is growing interest in the relationship between smart charging and the performance of on-board EV chargers [18]. For AC charging specifically, the behavior of the EV load is largely determined by the on-board charger [19], making performance metrics like power factor, efficiency, and harmonic distortion increasingly important.

While power factor and efficiency have been extensively studied in [20], which evaluated more than 35 different EV models, the effects of smart charging on harmonic distortion remain underexplored. Previous research has highlighted a negative correlation between charging current and both power factor and efficiency, pointing to the need for a deeper investigation into the harmonic content generated during smart EV charging. The rise in harmonic content due to smart EV charging is contributing to increased harmonic distortion within power networks, adversely affecting power quality. If total harmonic distortion exceeds industry standards, this form of electrical pollution can lead to serious complications. Left unchecked, harmonic distortion can result in the degradation of EV power cables, overheating of transformers, voltage instability, and heightened electromagnetic emissions, which may interfere with surrounding equipment [21], [22]. This study aims to fill this gap by analyzing the harmonic performance of on-board chargers across various smart charging current setpoints.

B. PROBLEM STATEMENT AND CONTRIBUTIONS

EVs are electrical loads that connect to the power grid via power electronics-based on-board chargers [23]. While smart charging is widely used to mitigate peak demand and improve voltage profiles, its impact on harmonic emissions remains insufficiently explored [20]. Current harmonic standards are typically designed for power electronic devices operating at single, fixed points (usually at rated power) [24], but smart charging introduces variability in operating points, which can significantly alter the harmonic behavior of on-board chargers, creating new power quality challenges [25]. Therefore, it is essential to investigate the relationship between smart charging current and the resulting harmonic content. In particular, there is a noticeable gap in the literature, as comprehensive datasets—such as those presented in Section II-B—that include both magnitudes and phase angles of harmonic currents at different smart charging rates are scarce. Such data are crucial for understanding the harmonic effects of single and multiple EV charging on power grid infrastructure.

The contributions of this paper are summarized as follows:

1) We present a detailed dataset on the harmonic emissions of eight different EV models across various smart charging rates. This dataset includes measurements from individual EVs as well as at the point of common coupling (PCC). Data collection was carried out using three distinct smart chargers and two types of power analyzers.
2) We perform a statistical analysis of key harmonic metrics, including current total harmonic distortion (THD_I), individual harmonic magnitudes, and phase angles, in relation to smart charging rates.
3) We assess the magnitude of individual EV harmonics against the IEC 61000-3-2 standard, highlighting any discrepancies related to THD_I.
4) We develop a Monte Carlo-based probabilistic approach to quantify the harmonic emissions from multiple EVs charging simultaneously. The simulation outcomes are compared to industry standards to better understand the cumulative effects of harmonic distortion.
5) We identify gaps in current industry standards regarding smart EV charging, propose areas for further research, and provide recommendations to enhance the implementation of smart charging technologies.

The structure of this paper is as follows. Section II provides a comprehensive review of the literature on smart EV charging, power quality concerns related to EV charging, existing harmonic datasets for EVs, and an overview of relevant industry standards. Section III describes the experimental setup, including the vehicles, chargers, and power quality analyzers used in this study. Section IV presents a statistical analysis of individual harmonic components (both magnitudes and phase angles) and discusses the relationship between THD_I and smart charging rates. Section V evaluates EV harmonic profiles against applicable industry standards for individual EV charging, while Section VI explores the harmonic emissions from multiple EVs charging simultaneously. Finally, Section VII summarizes the key findings and offers recommendations for future research.

TABLE 1. Restrictions for Current Harmonics in IEC 61000-3-2 [59]

Harmonic order (n)	Maximum permissible harmonic current (A)
Odd Harmonics	
3	2.30
5	1.14
7	0.77
9	0.40
11	0.33
13	0.21
$15 \leq n \leq 39$	0.15 x (15/n)
Even Harmonics	
2	1.08
4	0.43
6	0.30
$8 \leq n \leq 40$	0.23 x (8/n)

TABLE 2. Restrictions for Current Harmonics in IEC 61000-3-12 [60]

Minimum RCSE	Admissible individual harmonic current I_h/I_{ref} (%)				Admissible harmonic parameters (%)	
	I_5	I_7	I_{11}	I_{13}	THC/I_{ref}	$PWHC/I_{ref}$
33	10.7	7.2	3.1	2	13	22
66	14	9	5	3	16	25
120	19	12	7	4	22	28
250	31	20	12	7	37	38
350+	40	25	15	10	48	46

RSCE - Short-circuit ratio; I_h - Harmonic current component; I_{ref} - Reference current; THC - Total Harmonic Current; PWHC - Partial Weighted Harmonic Current

II. LITERATURE REVIEW

The literature can broadly be summarized under three subcategories: i) EV smart charging and its impacts on power grids; ii) existing harmonic measurement studies and impact assessment; and iii) associated industry standards. The following subsections provide a detailed review of each topic.

A. EV SMART CHARGING AND POWER-GRID IMPACTS

Smart charging of EVs is necessary to manage increasing EV demand within an already constrained power network [26]. Smart charging aims to capitalize on the flexibility of EV loads by employing one of the following methods [20]:

- **Modulation** of charging current within the minimum and maximum allowable charging currents (see Table 3 for sample data).
- **Scheduling** or turning on/off the charger.
- **Shifting**/changing the phase of the charger for three-phase balancing.
- **Phase curtailment** (from three phases to single phase) to increase the efficiency of charging.

Smart charging offers a wide range of benefits to different stakeholders. EV owners can benefit from reduced charging costs under the right market conditions by shifting their demand to off-peak hours. Similarly, increased EV hosting capacity, higher utilization of grid assets, and deferred grid reinforcements can be beneficial to grid operators [27], [28].

The impacts of uncontrolled EV charging on power grids have been well documented in numerous literature surveys (e.g., [14], [29]). Beyond literature surveys, studies aim to quantify the impacts of EV charging at generation, transmission, and distribution levels [26], [30]. At the generation level, many studies aim to estimate the additional EV load on the power grid typically by using stochastic Monte Carlo methods. For instance, in Germany, peak demand is expected to grow by one-fifth by 2050 due to EV charging [31]. In the U.K., 19 TWh of extra energy is needed to meet EV demand by 2035 if one-third of the nation's fleet is electrified [32]. Smart charging is considered a key method to reduce peak loading by shifting domestic EV charging to off-peak hours. For instance, the U.K. smart charging regulations [12] mandate that charging units should only be operational during off-peak hours, defined as (1) outside of 4 pm–10 pm on weekdays and (2) outside of 8 am–11 am on weekends.

At the distribution level, the primary focus is on the voltage drops stemming from domestic EV charging and developing strategies to minimize voltage violations [15], [33]. Higher shares of EV penetration will require transformer and feeder upgrades. According to a study conducted for California [34], by 2035, there will be a significant demand for infrastructure upgrades in 50% of feeders, increasing to 67% by 2045. Similarly, the distribution system requires a capacity increase of 25 GW by 2045, necessitating an investment ranging from $6 to $ 20 billion.

In [35], a smart charging framework is proposed to reduce the peak loading of the local transformer. However, this study does not include the harmonic levels when the charging currents reduce during smart charging. Overall, harmonic assessment of charging stations is critical for grid operators to manage new connection requests, and detailed analysis should be carried out using a data-driven approach [36].

B. HARMONIC IMPACT ASSESSMENT AND EXISTING DATASETS

This section presents EV charging harmonic impacts, a review of existing harmonic measurement studies, and methods to examine the harmonic impact of single and multiple EVs charging simultaneously. Non-linear loads, such as EV chargers, produce harmonics. The power electronics involved in EV charging inject current and voltage harmonics into the power grid due to the non-linear switching during the AC to DC power conversion [37]. Harmonic distortion significantly impacts power quality, especially with the increasing number of EV charging sessions. This type of electrical network pollution can become problematic if the total harmonic contents exceed the thresholds set by industry standards [38].

Harmonic distortion negatively impacts distribution network elements, including cables, transformers, switchgear, and customer equipment [39]. In cables, harmonics increase resistive losses, causing overheating and accelerating insulation degradation, which shortens the cable's lifespan if not

TABLE 3. Overview of Technical Specifications for EVs Used in the Experiments

EV Model	Model Year	On-board Battery Charger	Nominal Battery Capacity (kWh)	Practical Charging Current Range (A)	Charging Type (AC)	Practical Charging Power Range (kW)	Harmonic Orders Measurement
Renault Zoe R90	2018	Integrated	44.1	5.91 to 31.10	3-ϕ	0.00 to 21.46	Until 31st
Peugeot e-208	2021	Dedicated	50	6.01 to 14.66	3-ϕ	4.15 to 10.12	Until 31st
Nissan Leaf e+	2022	Dedicated	62	5.90 to 28.39	1-ϕ	1.36 to 6.530	Until 49th
VW ID.3 Pro	2023	Dedicated	62	6.09 to 15.86	3-ϕ	4.20 to 10.94	Until 31st
Renault Zoe ZE50	2022	Integrated	54.7	6.68 to 30.32	3-ϕ	3.08 to 20.92	Until 49th
VW ID.4 Pro	2024	Dedicated	82	6.06 to 15.67	3-ϕ	4.18 to 10.81	Until 49th
Tesla Model Y Long Range	2022	Dedicated	78.1	6.09 to 16.15	3-ϕ	4.20 to 11.14	Until 49th
Peugeot e-2008	2022	Dedicated	50	5.83 to 15.23	3-ϕ	4.02 to 10.51	Until 49th

properly rated [33], [40]. Transformers, on the other hand, suffer from higher eddy current losses and core saturation due to harmonics, resulting in excessive heat and reduced efficiency. This can potentially cause voltage irregularities and premature failure [21]. Additionally, harmonics can cause distortion in the magnetic flux, leading to core saturation, which further reduces the transformer's lifespan and increases the risk of voltage irregularities in the network [22]. The relationship between transformer efficiency and the K-value, an index of a transformer's ability to withstand harmonic currents, is crucial in determining the transformer's lifespan. Higher K-values result in increased thermal stress, potentially reducing the device's operational longevity. This relationship is expressed through a quadratic correlation linking the harmonic order and magnitude to the transformer's K-value [41]. The approach to quantify transformer loss of life is outlined in IEEE Standard C57.91 [42].

Switchgear components, such as circuit breakers, are also vulnerable to the impacts of harmonic distortion, thermal stress and nuisance tripping, which reduce their operational life [43]. For customer equipment, harmonics can cause overheating, voltage irregularities, and electromagnetic interference, leading to malfunctions, reduced efficiency, and potential damage to sensitive electronics. Furthermore, the increased electromagnetic interference caused by harmonic distortion poses a significant risk to on-board vehicle systems [44]. Without proper management, harmonic distortion weakens insulation, shortens the lifespan of network components, and compromises system reliability.

In the dynamic landscape of electric mobility, the on-board EV chargers have undergone significant upgrades since the late 2000s. While early chargers provided a basic charging service (converting AC to DC), modern on-board chargers provide higher efficiency and charging power, support bi-directional charging, and enable smart charging [45]. Therefore, this section focuses mainly on the main studies published in the last decade.

In one of the early harmonic measurement studies presented in [46], the harmonic measurement time series of an EV is recorded for a range of initial and final state of charge values. A probabilistic methodology is presented to evaluate two EVs charging, and individual harmonic effects are evaluated. The results show that when EV charging is in the second phase of the constant current-constant voltage (CC-CV) charging phase, the harmonic content increases significantly with reducing the charging current, leading to an increase in THD_I. Accompanying this paper is a partial dataset that includes odd harmonics at selected states of charge levels (fundamental and even harmonic information are excluded).

In [47], harmonic testing of 18 EV models (models earlier than 2016) was conducted using AC level 2 chargers with, predominantly, single-phase on-board chargers. The THD_I of EVs ranged between 1.7% and 11.9%, representing little sign of standardization. The paper further analyzed 3rd, 5th, and 7th individual harmonics and associated phase angles to gain insight into cancellation effects. Updated vehicle charging profiles are required to assess whether a reduction in harmonic emissions has been observed since this study in 2016.

In [36], harmonic measurements of 23 different EVs are presented using slow AC chargers ranging from 2.3 kW to 7.2 kW. In this study, only the magnitude of individual harmonics was measured, and harmonic cancellation was ignored. This work attempts to compute the harmonic hosting capacity of rural and urban power networks in the U.K. by proposing a probabilistic simulation technique. In [48], harmonic measurements are taken from DC charging and bi-directional discharging of a Nissan Leaf at 2, 5, and 10 kW charging rates. Individual harmonics are examined using the IEEE 519-2014 standard [49].

A more recent study [50] presents measurements of EV charging profiles for 12 different EVs, including both pure electric and plug-in hybrid vehicles. The dataset includes active power (kW), reactive power (kVAR), apparent power (kVA), voltage (V rms), current (A rms), and both voltage and current harmonics. Each EV is charged for several hours using level-2 chargers rated at 6.6 kW. Smart charging is not applied during any of the charging sessions. The results show that the total harmonic and demand distortion, in most cases, do not exceed the associated industry limits.

In [51], the current harmonic measurements are taken at the PCC at an EV charging station. Since there was only one measurement point, detailed information on vehicle types and charge levels is unknown. The statistical behavior of the third harmonic is primarily investigated, as this component represented the highest harmonic content. The results show that the maximum active charging power of the station is

around 60 kW, while the associated total demand distortion has exceeded 10%. In [25], a specific focus is given to supra-harmonics (harmonics greater than 50 kHz) for varying charging currents. It was concluded that EV chargers are a source of supra-harmonic emissions, and standardization efforts are needed to address associated issues.

Until recently, most harmonic studies lacked the recording of phase angles due to technical limitations in recording devices. To address this lack of phase angle data, the IEC proposed a summation law that approximates harmonic sums without considering phase angles [52]. The summation effect of harmonic currents is given as below [53]

$$(I)^{\alpha}_{h,\Sigma} = \sum i^{N_d} (I)^{\alpha}_{h,i},$$

where, α is the summation coefficient for hth harmonic order, $I^{\alpha}h$, Σ is the 95% non-exceeding probability values of the total current, $I^{\alpha}_{h,i}$ denotes the 95% non-exceeding probability value of the load i, and N_d is the total number of loads (it is the number of EVs in case of smart charging). The IEC standard [53] determines the summation coefficients as follows. For harmonic orders less than five, that is $h < 5$, α equals to 1. For harmonic orders higher than ten ($h > 10$), $\alpha = 2$. For other harmonic orders, it is set as 1.4. This method is mostly applied to non-EV loads. For instance, [54] demonstrates that the summation coefficients, calculated using data from multiple arc furnace sites, are sensitive to the chosen probability threshold and calculation interval, which affect the degree of random variation in harmonic voltages/currents. In [55], coefficients up to the 20th order are calculated for a railway rectifier between 1.8–2.0. Additionally, [56] indicates that wind farm topology and assumptions about magnitude/phase angle distributions can influence summation coefficients.

In [57], the influence of harmonic current cancellation on the combined effect of various load currents is assessed to demonstrate its network impact by comparing measured and mathematically aggregated harmonics. Additionally, the harmonic cancellation phenomenon is quantified for multiple loads connected to the power supply. [57] further computes the harmonic cancellation effect of uncontrolled EV charging using data from [58]. It was shown that the cancellation coefficient distributions for EV charging loads are wider than those for LED lamps. This difference is due to the dissimilar harmonic current profiles exhibited by these two load types.

The review presented in this section demonstrates that existing datasets and analyses fail to provide an in-depth analysis of the complex relationship between smart charging and the associated harmonic emissions. Current studies often lack the granularity (especially in phase angles) and comprehensive scope to account for the variability and interaction of harmonics generated by different EV chargers operating simultaneously under diverse conditions. This insufficiency in data and analysis limits our understanding of how smart charging strategies impact harmonic levels, which is crucial for maintaining power quality and grid stability. In real-world scenarios, the harmonic profile of multiple EVs charging simultaneously depends on the specific vehicle types and their concurrent charging rates (e.g., 6–16 amps). Given the potentially vast number of combinations of EV types and charging rates, a probabilistic simulation approach is the most suitable method for calculating the probability of exceeding established industry limits. These methods should leverage detailed harmonic information and account for various factors, including charger types, charging patterns, grid configurations, and the stochastic nature of EV charging behaviors. By adopting a probabilistic approach, researchers and grid operators can better predict and manage the harmonic impacts of widespread EV adoption, ensuring more reliable and efficient integration of EVs into the power grid.

C. INDUSTRY STANDARDS FOR HARMONIC LIMITATION

The International Electrotechnical Commission (IEC), the European Committee for Electrotechnical Standardization (CENELEC), and the Institute of Electrical and Electronics Engineers (IEEE) are institutions that define widely adopted power quality standards. The relevant standards for this analysis are identified as follows.

- **The IEC 61000** identifies certain types of disturbances and their characteristics and measurement methodologies. EV chargers must meet the electromagnetic compatibility IEC 61000 series standards for loads connected to a power grid. These standards define the harmonic emission levels, such as the harmonic current-voltage or power factor that an EV charger is permitted to have. IEC 61000-3-2 [59] (rated current $\leq$ 16A) and IEC 61000-3-12 [60] (rated current $>$ 16A) are the standards applicable to EV chargers and set limitations on current harmonic emissions that EV chargers inject into the grid, while IEC 61000-2-2 [61], which covers low-frequency disturbances in public networks, and IEC 61000-2-4 [62], which covers low-frequency disturbances in industrial and non-public networks, set limitations on voltage harmonic emissions. The IEC 61000-4-7 [63] and IEC 61000-4-30 [64] standards handle these harmonic measurements and instrumentation.
- **The European Norm (EN) 50160** [65] sets the voltage limits for network operators established by the CENELEC. EN 50160 defines the voltage distortion limits that the network operator must comply with in LV and MV electrical distribution networks. It also defines the main voltage parameters at the consumer's PCC and their allowable deviation range.
- **IEEE 519-2014** [49] provides recommendations for voltage and current distortion limits for network operators and users, respectively.

These standards, which outline the problems that harmonic distortions cause in power systems and the degree of tolerability of harmonics, have been widely adopted by industry and academia.

In this study, two types of EV charging are considered. The first type aims to emulate domestic EV charging, which draws

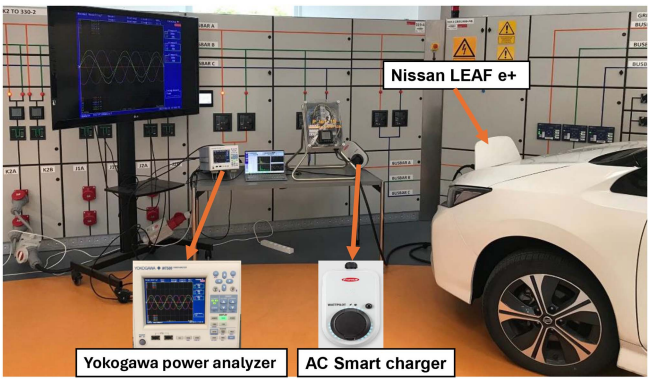

FIGURE 1. Overview of the experimental set-up and laboratory environment.

less than 16A per phase. The second case emulates a public charging station, and it is assumed that per-phase charging is higher than 16A. Therefore, IEC 61000-3-2 and IEC 61000-3-12 standards are used in our evaluations. A summary of relevant details from these standards is given in Tables 1 and 2, respectively.

III. EXPERIMENTAL SET-UP

The EV smart charging experiments documented in this paper were carried out at the Energy System Integration Lab (SYS-LAB) at the Technical University of Denmark (DTU) [66]. Eight distinct battery EVs, namely, Renault Zoe R90, Peugeot e-208, Nissan Leaf e+, VW ID.3 Pro, Renault Zoe ZE50, VW ID.4 Pro, Tesla Model Y Long Range, and Peugeot e-2008 were tested.[1] The rationale behind the selection process is to capture the current market shares and diversity in model year, battery capacity and all on-board charger characteristics. The technical details of the vehicles tested are presented in Table 3. The average age of vehicles was less than two years at the time of the test. Hence, the majority of vehicles tested have a larger battery capacity than those examined elsewhere in the literature (see Section II-B). Moreover, Fig. 1 shows the experimental setup for a single EV charging case. The charging devices and power quality analyzers used in this experiment are described in detail in this section.

The EVs used in these experiments have a range of on-board charger technologies. For example, both Renault Zoe models have integrated on-board chargers, while other vehicles have dedicated on-board charging. The technology differences of on-board chargers have been thoroughly explained in [68]. Integrated battery charging refers to a system in which the charging components, such as the charger and inverter, are built directly into the vehicle's electric motor. In this setup, the vehicle's on-board charger converts AC power from an external power source (e.g., a charging station or wall outlet) into DC power to charge the battery. A dedicated battery on-board charger requires separate components

[1]Data is publicly available on [67].

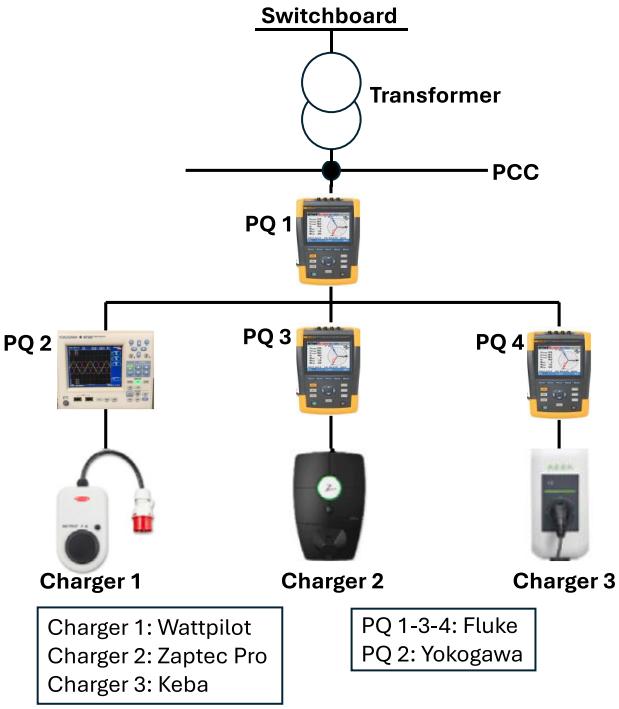

FIGURE 2. Arrangement for an experiment involving smart chargers and power quality analyzers.

and does not share any modules with the vehicle. This unit converts AC power from the external source into DC power suitable for charging the EV battery. This type of charging system can offer flexibility in terms of charging speed and can support faster charging rates depending on the capabilities of the external charging unit.

The AC smart chargers used for these experiments are Fronius Wattpilot [69], Zaptec Pro [70], and Keba KeContact P30 [71]. All smart chargers are three-phase and are capable of up to 32A per phase, schedule charging (on/off), and modulate charging (up/down). Wattpilot and Keba use mobile applications, Solar.wattpilot and Keba eMobility App, respectively, to issue setpoints while the Zaptec Pro uses a web-based portal. Harmonics measurement was recorded either with a Yokogawa WT500 power analyzer [72] or a Fluke 437 Series II power quality analyzer device [73]. At the time of the experiments, all measurement devices were recently calibrated and certified to ensure the accuracy of the collected data. Depending on the functionality of these devices, harmonic orders were measured up to 31st or 49th. In this experiment, one Yokogawa and three Fluke devices were used. Fig. 2 shows the charging diagram for an experiment. Since the Yokogawa power analyzer can measure up to 40A, a Fluke device was configured to measure current up to 100A at the PCC.

The vehicles were charged at 1A granularity within the minimum and maximum charging current range to emulate practical smart charging applications. According to the IEC 61851-1 standard [74], EVs cannot charge with currents lower than 6A. Maximum charging rates are determined by both

the IEC 61851-1 standard and the technological limitations imposed by the battery management system and the vehicle on-board charger [20]. Although practical charging currents may vary, the maximum charging current can be either 16A or 32A, depending on the EV, as seen from Table 3. It should be noted that two types of measurements were carried out. The first is designed to characterize the harmonics profile of individual EVs. In this case, Charger 1 (Wattpilot, due to ease of configuration) was connected to each vehicle, and harmonic content was measured from the minimum to the maximum charging rates. In the second set of experiments, all three chargers were connected to different vehicles, and measurements of the individual and PCC levels were taken.

IV. STATISTICAL DATA ANALYSIS

Charging data, including root mean square (RMS) charging current (A), RMS voltage (V) of the charging outlet, fundamental current and voltage, as well as individual harmonic orders with their corresponding amplitude and phase angle (in degrees) for both voltage and current, were collected using a power analyzer. Sampling occurred every second, facilitated by the connection between the power quality analyzer device and a dedicated workstation computer.

A. THD ANALYSIS

THD is a metric used to quantify the degree of distortion of current or voltage compared to their ideal waveform. It indicates the relative signal energy at frequencies beyond the fundamental frequency [75]. The THD for current and voltage harmonics is calculated as follows:

$$\mathrm{THD}_I = \frac{\sqrt{\sum_{h=2}^{H} I_h^2}}{I_1} \times 100\%, \tag{1}$$

and

$$\mathrm{THD}_V = \frac{\sqrt{\sum_{h=2}^{H} V_h^2}}{V_1} \times 100\%, \tag{2}$$

where $I_{h\in\{2,3,4\ldots\}}$ and $V_{h\in\{2,3,4\ldots\}}$ represent the RMS value of the h^{th} individual harmonic order, H is the maximum harmonic order and I_1 and V_1 represent the fundamental current and voltage, respectively. THD values were acquired every second during EV charging using a power quality analyzer.

To simulate smart charging conditions, each EV was charged within the minimum and maximum charging current range with decrements of 1A (only VW ID.3 Pro has 2A intervals due to this vehicle's limited availability during testing). Fig. 3 shows time series measurements of $\mathrm{THD_I}$-smart charging for eight different EVs. From these results, several observations can be enumerated as follows:

1) $\mathrm{THD_I}$ has its lowest value when the vehicle is charged at its maximum rate, implying that the on-board chargers are designed to operate at the rated capacity.
2) The $\mathrm{THD_I}$ and the charging rate are inversely proportional. At lower charging rates, the $\mathrm{THD_I}$ increases significantly - by more than threefold in most tested vehicles.
3) The ramp rate of vehicles' response times to changing charging rates varies. It can be seen from Fig. 3 that certain vehicles (e.g., Peugeot e-208 and VW ID.3 Pro) can show rapid responses to changes in charging current, while the response delay is longer for other vehicles (e.g., Peugeot e-2008) [68]. While this is not a significant issue for harmonic emission, response times are of critical importance for vehicle-to-grid applications [68].

TABLE 4. Correlation Coefficient (r) and Quadratic Polynomial Parameters ($f(x) = p_1x^2 + p_2x + p_3$) Between $\mathrm{I_{Charge}}/\mathrm{I_{Max}}$ and $\mathrm{THD_I}$(%)

EV Model	r	p_1	p_2	p_3	R^2
Renault Zoe R90	-0.94	13.91	-25.08	16.14	0.97
Peugeot e-208	-0.89	11.06	-19.85	11.42	0.86
Nissan Leaf e+	-0.79	22.01	-30.63	13.98	0.92
VW ID.3 Pro	-0.92	9.889	-17.03	9.363	0.97
Renault Zoe ZE50	-0.87	26.05	-38.71	18.92	0.97
VW ID.4 Pro	-0.85	11.68	-19.36	10.28	0.92
Tesla Model Y LR	-0.95	13.6	-26.37	18.07	0.99
Peugeot e-2008	-0.98	26.25	-58.01	42.74	0.99

R^2 denotes the R-squared statistics.

Let I_{Charge} denote the per-phase charging current of a vehicle and I_{Max} denote the maximum charging rate (see practical charging rate column in Table 3). Since there are two groups of I_{Max} (around 16A and 32A), the charging current of each vehicle is normalized as $I_{\mathrm{Charge}}/I_{\mathrm{Max}}$ and plotted against the $\mathrm{THD_I}$ (%) as shown in Fig. 4. Only VW ID.3 Pro and VW ID.4 Pro have a harmonic content that is less than 5% for all charging currents. Peugeot e-2008 has the highest emission content, whilst all other EVs have $\mathrm{THD_I}$ content between 5% and 14%.

To further investigate $\mathrm{THD_I}$ (charging current relationship), the correlation coefficients are calculated and presented in Table 4. The correlation coefficient is a statistical measure that quantifies the strength and direction of the linear relationship between two variables. It ranges from -1 to $+1$. A value of $+1$ implies a perfect positive linear relationship. Conversely, -1 indicates a perfect negative linear relationship, and 0 indicates no linear relationship between the variables [76]. The results show a strong negative correlation, as seven out of eight EVs have a correlation coefficient between -0.85 and -0.99. Nissan Leaf e+ has a correlation coefficient of -0.79. This correlation is due to the $\mathrm{THD_I}$ (%) being consistent until 10A of charging, as shown in Fig. 3. Given the high correlation between the two parameters, quadratic regression ($f(x) = p_1x^2 + p_2x + p_3$) is applied to all EV types and polynomial coefficients are calculated along with R-squared statistics and presented in Table 4. This polynomial regression may be considered in future research to represent $\mathrm{THD_I}$ as a function of charging current, which could be used as a constraint in individual EV optimization problems. Additionally, polynomial values could provide good estimates of non-integer charging rates. For instance, if a Tesla Model Y has a charging power

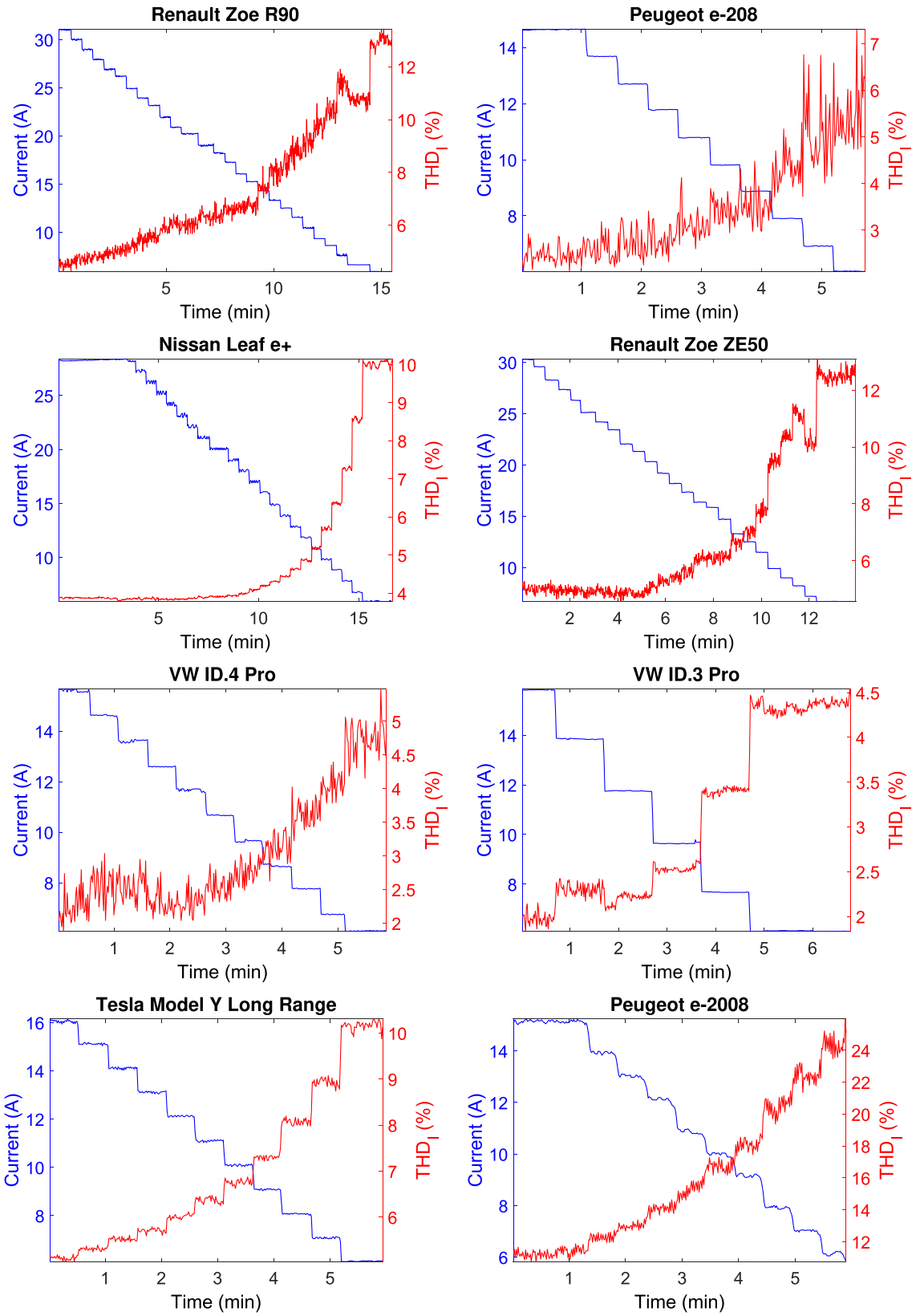

FIGURE 3. THD_I (%) versus charging rate for all EVs.

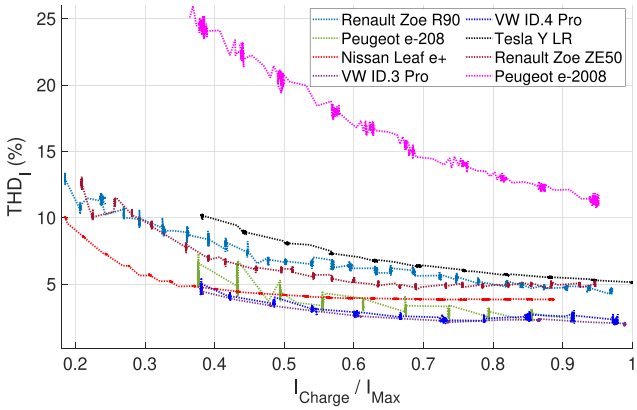

FIGURE 4. Correlation between I_{charge}/I_{max} and THD_I (%).

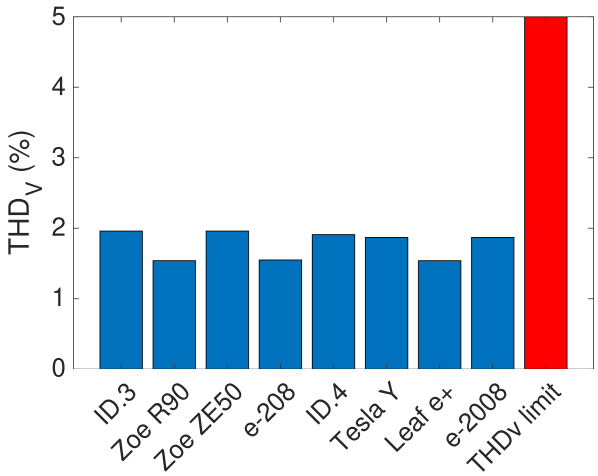

FIGURE 5. 75th percentiles of THD_V (%) for all EVs during smart charging.

of 10.5A, the associated THD_I (%) emission would be

$$f\left(\frac{10.5}{16.15}\right) = 13.6 \times \left(\frac{10.5}{16.15}\right)^2 - 26.37 \times \left(\frac{10.5}{16.15}\right) + 18.7 = 7.3\%.$$

In this calculation, $I_{\text{Charge}} = 10.5\text{A}$ and $I_{\text{Max}} = 16.15\text{A}$.

Next, voltage total harmonic distortion (THD_V) occurring during the smart charging is presented. Fig. 5 shows the 75th percentiles of THD_V (%) for all EVs and related THD_V limitation. Unlike THD_I, the 75th percentiles of THD_V values varies in a minimal range (between 1.5% and 2%), independent of the smart charging current rate for all EVs. More importantly, THD_V consistently stays below industry limits as per IEC 61000-2-4 [62], with 5% set as a limit for class 1, protected supplies, and IEEE 519-2014 [49] with 8% set as the limit for low voltages (below 1kV).

In addition to assessing voltage harmonics during EV charging, their impact was further investigated by measuring them both before and during the charging process. Fig. 6 illustrates the THD_V for a Nissan Leaf e+ in both scenarios. The findings revealed no correlation between EV charging and

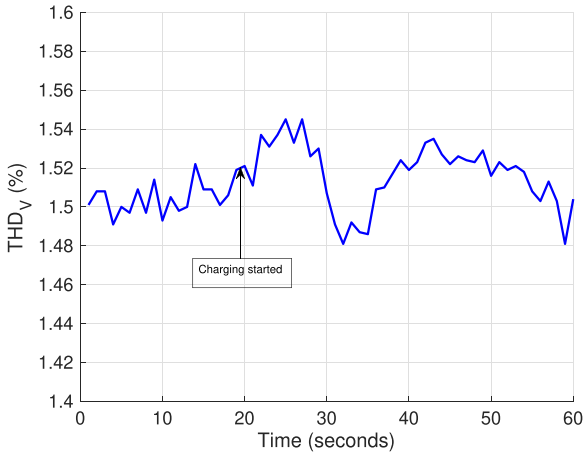

FIGURE 6. THD_V assessment before and during charging.

THD_V, indicating that voltage harmonics are generated from the supply side rather than the load side. Thus, the observed voltage harmonics were due to background distortion rather than the charging process itself. Consequently, the subsequent focus in this paper is directed toward analysing current harmonics.

B. AMPLITUDE ANALYSIS

The amplitudes of individual harmonics play a crucial role in calculating THD_I and determining the limits outlined in power quality standards. These measurements were taken every second as a time series and averaged over one-minute intervals. Fig. 7 shows the heatmap of the amplitudes of the individual harmonics for all EVs. In the previous section, the negative correlation between charging current and THD_I was established. However, the relationship between individual current harmonic orders against the charging current is outlined in Fig. 7, where such correlations are not observed. For instance, there are individual harmonics whose amplitude increases with increasing current (e.g., 2nd harmonic order in VW ID.3 Pro and VW ID.4 Pro), while there are also individual harmonics whose amplitude decreases with increasing current (e.g., 17th harmonic order in Renault Zoe R90). Additionally, some harmonics do not exhibit any noticeable pattern with a change in charging current.

When assessing different harmonic orders for the same vehicle, it is observed that the 7th harmonic order has the highest magnitude, regardless of the charging current. In addition to the 7th harmonic, the 3rd and 5th harmonics also stand out due to their larger amplitudes in comparison with other harmonic orders. As discussed in Section II, existing research predominantly focuses on 3rd, 5th and 7th harmonics due to their significance. It can be seen from Fig. 7 that these harmonic components represent the highest harmonic magnitudes in all vehicles. It is also important to consider phase angles of high-amplitude harmonics, particularly when multiple EVs charge simultaneously. Phase angles of high-magnitude harmonics will ultimately determine whether they reinforce or cancel each other during concurrent EV charging.

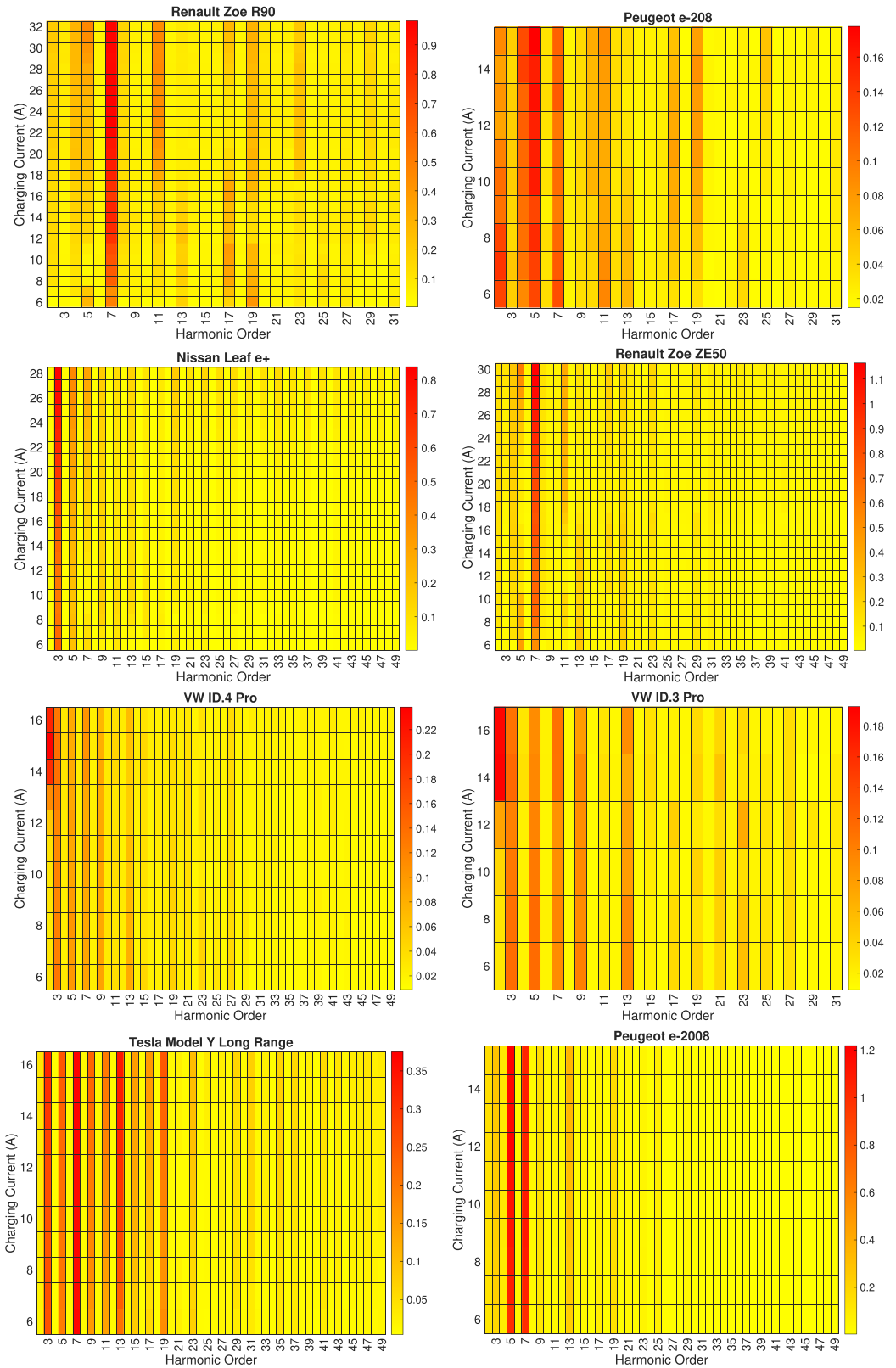

FIGURE 7. Individual current harmonics amplitude (A) for all EVs.

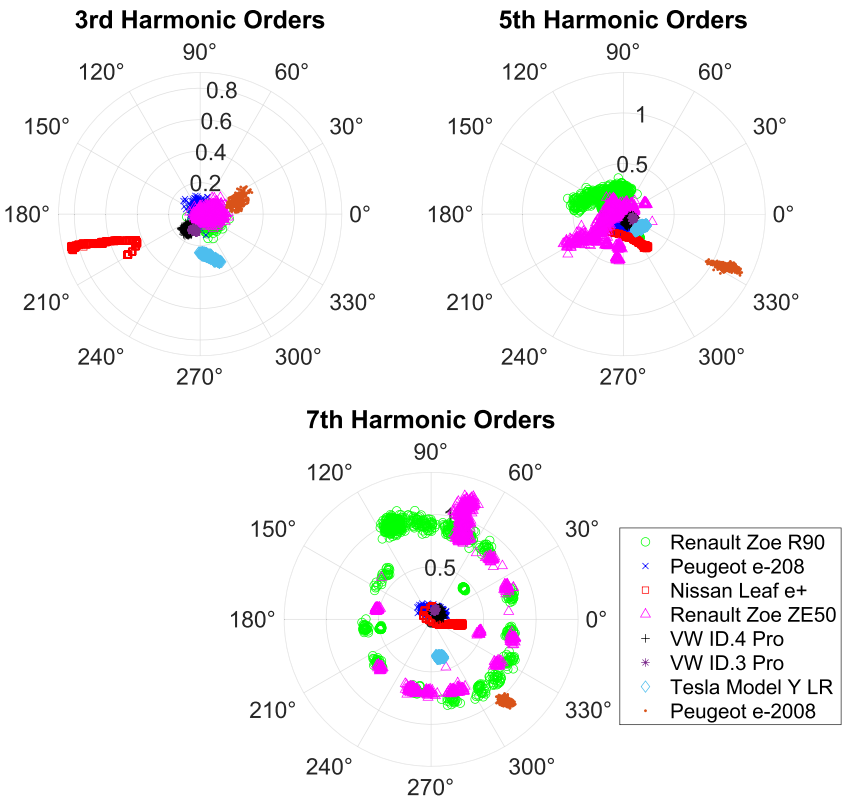

FIGURE 8. Phase angles of (in degrees) 3rd, 5th and 7th harmonic orders for all EVs.

C. PHASE ANGLE ANALYSIS

Harmonic orders, as with fundamental currents and voltages, are depicted in a complex form requiring both amplitude and phase angle information. The consideration of phase angles is, therefore, an important element of harmonic analysis. Considering the individual harmonics of all EVs, the amplitudes of the 5th, 7th, and 9th harmonics are more significant than the others, revealing the importance of further investigation of these harmonics. While the amplitudes of these harmonics are significant compared to power quality standards, the phase angles are also required as they indicate whether the sum of harmonics will cancel or intensify each other. Due to the variation in phase angles for the same harmonic order for different vehicles, the sum of concurrent charging EVs will be lower than the arithmetical sum of their individual amplitudes. Should more than one EV of the same type charge at the same rate, then their sum will be equal to their arithmetical sum.

The polar plot of these harmonics (3rd, 5th, and 7th) is shown in Fig. 8. The aim is to investigate whether the harmonic distribution of EVs is widely dispersed for the same harmonic orders at different charging rates. For instance, while the individual harmonics of the Peugeot e-2008 are concentrated in certain parts, it is evident from Fig. 8 that the harmonics of vehicles such as the Renault Zoe R90 and Nissan Leaf e+ are more widely distributed. It is observed that the 3rd harmonics of the Peugeot e-2008 reside between 0 and 30 degrees while the Nissan Leaf e+ range between 180 and 210 degrees for the same order. An element of harmonic cancellation between these vehicles will be observed, given the 180-degree difference between their phase angles.

TABLE 5. Circular Descriptive Statistics for Phase Angles (In degrees) [77]

Charging Current (A)	Harmonic Order					
	3		5		7	
	Mean	Variance	Mean	Variance	Mean	Variance
6	-117.3	13.4	-73.9	13.6	92.9	37.8
7	-66.5	36.7	-92.9	37.8	17.2	26.4
8	-91.9	38.3	-77.7	17.6	70.0	44.6
9	-89.9	42.3	-77.7	12.7	-110.4	48.8
10	-105.6	36.3	-57.1	11.3	-15.1	50.0
11	-123.7	47.8	-63.3	25.4	-62.7	31.7
12	-123.9	35.8	-39.4	30.8	-15.4	38.7
13	-120.7	43.7	-51.8	38.3	-45.4	29.4
14	-115.3	29.8	-32.7	31.1	-4.2	33.1
15	-42.1	48.5	-54.2	32.4	-27.3	31.5
16	-113.8	17.2	-17.0	34.7	5.8	18.7

Moreover, circular data analysis is presented to analyze the behavior of phase angles beyond graphical representation. Note that conventional descriptive statistics (e.g., sample mean, variance) cannot be applied to angular values. For instance, consider two harmonic contents with angular values of 1 and 359. The sample mean would be 180; however, the angular mean is 0 degrees. Therefore, the mean and variance are calculated using MATLAB functions via [77]. Table 5 presents the mean and variance for the 3rd, 5th, and 7th harmonic orders across charging currents ranging from 6A to 16A. In this analysis, individual vehicles are not considered

separately; instead, all phase angles are collectively examined to determine their mean and variance, assessing the potential for cancellation effects. The results indicate that the 3rd, 5th, and 7th harmonic order variance ranges from 10 to 50 angular degrees (as indicated in Table 5). Therefore, in scenarios involving multiple EVs charging at the same rate, the resulting new harmonic content is expected to be slightly less than the arithmetic sum of each vehicle, and exact cancellation is improbable.

V. POWER QUALITY ASSESSMENT-SINGLE EV CHARGING

The power quality assessment for both single and multiple EV charging cases involves examining harmonic content relative to industry standards (details are given in Section II-C). For single EV charging, the process is straightforward and entails comparing individual harmonics to maximum allowable levels. However, assessing the simultaneous charging of multiple EVs introduces complexities. First, the vector summation of individual harmonics requires consideration of both harmonic magnitudes and phase angles. Second, as the number of EVs charging simultaneously increases, the variety of possible combinations of EV types and charging states grows significantly, necessitating a probabilistic approach to assess these scenarios.

The IEC 61000-3-2 is a widely used industry standard for single EV charging (details given in Table 1), providing maximum current levels for individual harmonics. Fig. 9 presents a heatmap for harmonic violations for all vehicles and all individual harmonic levels. It is observed that four out of eight vehicles measured in the experiments, namely the Renault Zoe R90, Renault Zoe ZE50, Tesla Model Y Long Range and Peugeot e-2008, exceed the threshold limits for several individual harmonics according to this standard. The 19th harmonic (950 Hz - likely the switching frequency of the onboard power electronics [78]) consistently exceeds the limits in all cases. However, the 7th harmonic, highlighted in the previous section for its significant amplitude, does not exceed the limits to the same extent as the 19th harmonic. This underlines the importance of considering lower-amplitude harmonics in power quality assessments.

Another observation is the similarity in THD_I behavior between the Tesla Model Y and the Nissan Leaf e+, with THD_I ranging between 4 and 10%. However, while no individual harmonic of the Nissan Leaf e+ exceeds the IEC 61000-3-2 limits, six different individual harmonics of the Tesla Model Y exceed the limits. Despite having a higher THD_I at low current, most of Tesla Model Y's harmonics, such as 17th, 23rd, 31st and 35th, exceed the limits at high current rather than at low current.

The findings in this section reveal contradictory outcomes regarding THD_I and specific harmonics. For instance, the lowest THD_I levels are observed when the charging power nears its maximum capacity (e.g., 16 Amps). However, with higher charging rates, there is a notable increase in the quantity of individual harmonic breaches compared to lower charging rates. Additionally, EVs exhibiting identical THD_I levels may demonstrate significantly different individual harmonic profiles and violations. For example, both the Tesla Model Y and the Nissan Leaf e+ exhibit a 10% THD_I during 6 Amp charging. However, while the Tesla Model Y shows individual harmonic violations, the Nissan Leaf e+ remains within harmonic limits.

TABLE 6. Charging Currents for Tesla Model Y Long Range, Renault Zoe R90, and Peugeot e-2008 Charging Simultaneously

Tesla Model Y Long Range (A)	Renault Zoe R90 (A)	Peugeot e-2008 (A)
6	6	6
9	9	9
12	12	12
15	15	15

VI. POWER QUALITY ASSESSMENT-MULTIPLE EV CHARGING

A critical aspect of practical harmonic studies is accurately representing harmonic-current summations. When several loads are connected to the same bus, the total harmonic current injected into the bus is the sum of all individual harmonic currents [79]. Since harmonic currents are represented by vectors, it is necessary to consider the magnitudes and phase angles of each individual vector to perform the vector summation. The diversity of devices with different circuit topologies can result in different current-harmonic phase angles, potentially causing a lower magnitude than the arithmetical sum of the harmonic currents [38]. The analysis of aggregated loads and the effects of cancellation or amplification of harmonic currents requires the consideration of the "absolute" harmonic phase angle, which is the angle between current harmonics and fundamental voltage, as specified in IEC 61000-3-12 [60]. This is distinct from harmonic power-flow studies, which require the "relative" harmonic phase angle, representing the angle between harmonic voltage and harmonic current.

Two studies are provided to evaluate the overall harmonics profile generated by multiple EVs. The first study offers laboratory measurements conducted on three EVs with different charging rates, whereas the second study employs a Monte Carlo simulation to analyze a broad range of EV charging scenarios across various charging rates.

A. LAB MEASUREMENTS CASE STUDY

This section presents an experimental study for harmonics emissions of three EVs charging simultaneously. Three power quality analyzers were allocated for each vehicle, and one power analyzer was used for PCC measurement. Based on the availability of the vehicles, Tesla Model Y Long Range, Renault Zoe R90, and Peugeot e-2008 were used in this charging setup as shown in Fig. 10. These vehicles were charged simultaneously with four different charging currents to emulate possible smart charging scenarios, given in Table 6. The THD_I and THD_V pattern, illustrating the variation in changing smart charging current, is depicted in Fig. 11. The pattern of

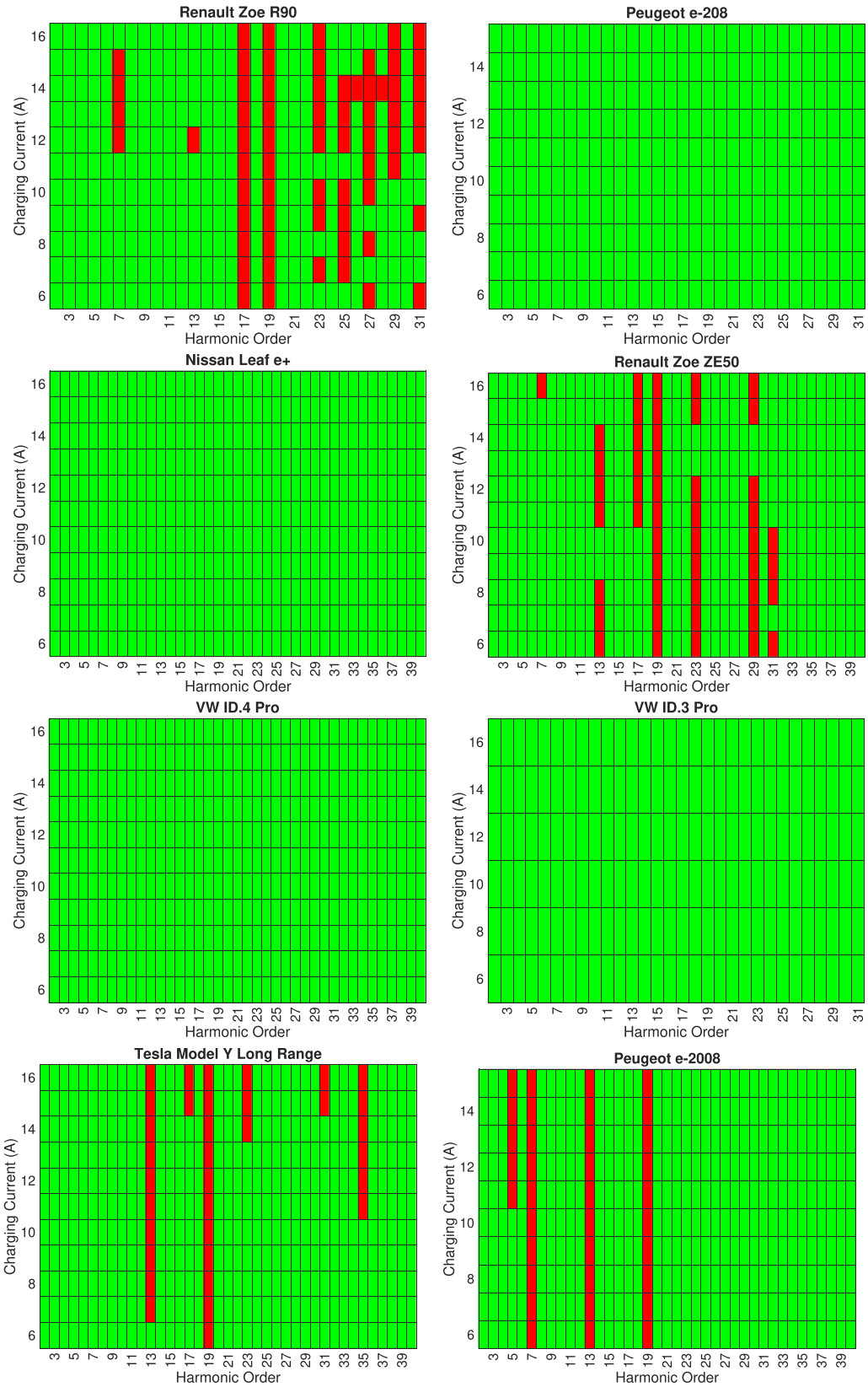

FIGURE 9. Violation of individual current harmonics against IEC-61000-3-2 standard for all EVs.

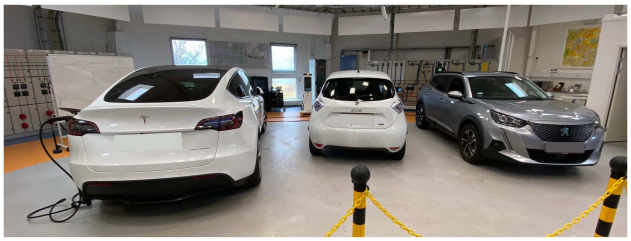

FIGURE 10. 3 EVs (Tesla Y Long Range, Renault Zoe R90 and Peugeot e-2008) charging simultaneously.

TABLE 7. Example for Harmonic Cancellation of Multiple EVs Charging

	Harmonic Orders (1st minute)					
	3		5		7	
	A	θ	A	θ	A	θ
Tesla Model Y LR	0.24	-83.6	0.09	-60.0	0.45	-73.5
Renault Zoe R90	0.23	152.1	4.08	0.98	10.56	87.3
Peugeot e-2008	3.35	47.3	7.92	-67.0	21.43	40.7
PCC	3.14	48.1	10.27	-45.3	29.42	54.9

A denotes amplitude and θ denotes phase angle in degrees.

decreasing THD_I with increasing current is evident. However, it is observed that smart charging does not impact voltage harmonics THD_V as THD_V of vehicles and PCC is always between 1.65% and 1.85%. This is well below the the THD_V limit of 5% as set out by IEC 61000-2-4. As mentioned in Fig. 6, EV charging does not affect harmonic voltage distortion.

Moreover, the simultaneous charging of the three vehicles plays a crucial role in cancelling out their individual harmonics, thereby reducing the THD_I at the PCC. The cancellation effect can be explained as follows: To perform the vector summation of the 3rd harmonic order for three EVs and the PCC, we treat each harmonic component as a phasor, represented by a complex number in polar form:

$$\text{Phasor} = A \cdot e^{j\theta},$$

where, A is the amplitude, θ is the phase angle in degrees and j is the imaginary unit ($j = \sqrt{-1}$).

To add phasors, we first convert them from polar form $A \cdot e^{j\theta}$ to rectangular form (real and imaginary components) using:

$$\text{Rectangular Form} = A \cdot (\cos(\theta) + j \sin(\theta))$$

Table 7 gives the amplitudes and phase angles of the 3rd, 5th, and 7th harmonics, a snapshot for the first minute from the charging vehicles and the PCC. Note that harmonic measurements were recorded each second during the charging process. For the 3rd harmonic order, amplitude (A) and phase angle (θ) are given in Table 7, such as $A = 0.24, \quad \theta = -83.6^\circ$ for Tesla Model Y LR. For each EV, the rectangular form is calculated as follows:

$$\text{Tesla Model Y LR:} \quad 0.24 \cdot \left(\cos(-83.6^\circ) + j \sin(-83.6^\circ)\right)$$

$$\text{Renault Zoe R90:} \quad 0.23 \cdot \left(\cos(152.1^\circ) + j \sin(152.1^\circ)\right)$$

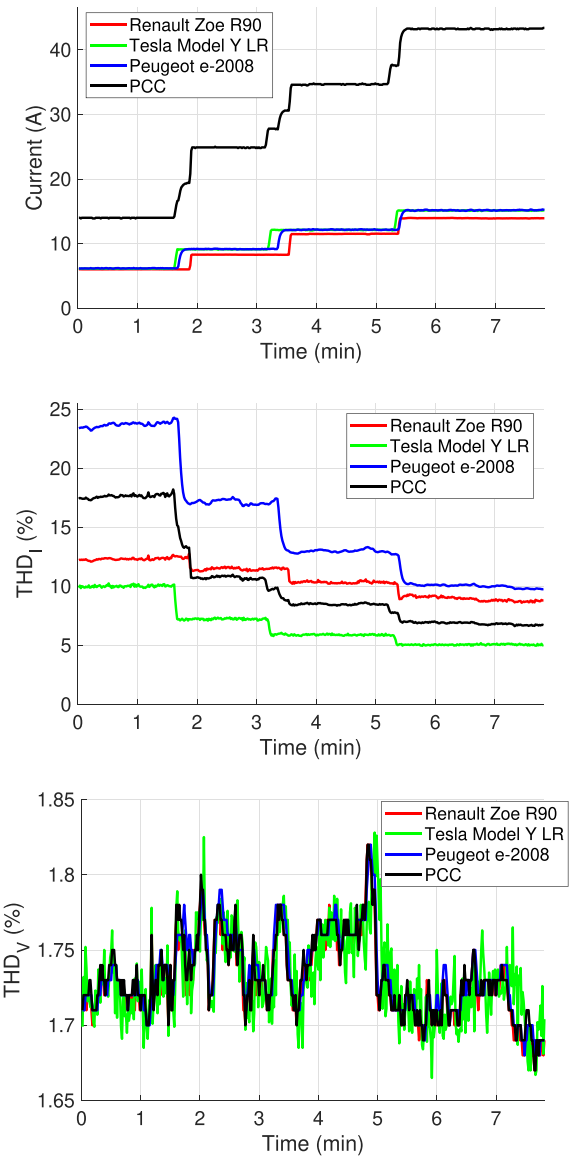

FIGURE 11. Measurement results of three EVs charging at the same time: [Top] Charging current vs. time, [Middle] Current harmonic distortion (THD_I) vs. time and [Bottom] Voltage harmonic distortion (THD_V) vs. time.

$$\text{Peugeot e-2008:} \quad 3.35 \cdot \left(\cos(47.3^\circ) + j \sin(47.3^\circ)\right)$$

We then sum the real and imaginary components of these three phasors to get the total phasor:

$$\text{Total Phasor} = \sum_{\text{EVs}} \text{Rectangular form of each EV}$$

This gives us a resultant phasor in rectangular form. The resultant phasor is converted back to polar form to find the combined amplitude and phase angle:

$$\text{Resultant Amplitude} = \sqrt{(\text{Real Part})^2 + (\text{Imaginary Part})^2}$$

$$\text{Resultant Phase Angle} = \tan^{-1}\left(\frac{\text{Imaginary Part}}{\text{Real Part}}\right)$$

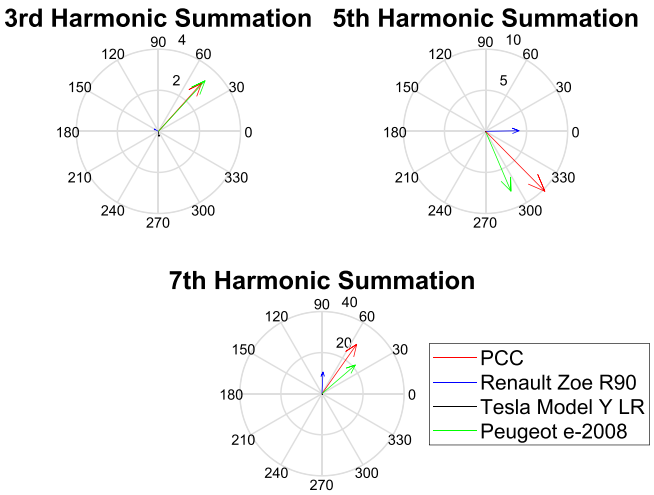

FIGURE 12. Example for harmonic vector summation of 3rd, 5th and 7th harmonic orders for multiple EVs charging.

Since the real part = 2.097, imaginary part = 2.337, the results for the summation of three EVs are:

$$A_{\text{PCC}} = 3.14, \quad \theta_{\text{PCC}} = 48.1^{\circ}$$

If there were no harmonic cancellation, A_{PCC} would be 3.82 $(0.24 + 0.23 + 3.35)$.

The mathematical representation of the sum of the 3rd harmonics, along with the vector sum of the 3rd, 5th, and 7th harmonics, is illustrated in Fig. 12. Although the PCC exhibits a higher amplitude for the summation of 5th and 7th harmonics compared to the amplitudes of individual vehicles, the amplitude of the Peugeot e-2008's 3rd harmonic surpasses that of the PCC. This observation underscores the significance of both the amplitude magnitudes and their positions on the coordinate plane (phase angle).

In this experiment, four different charging scenarios led to four distinct stages. In the first charging scenario (6A-6A-6A charging simultaneously), the THD_I at the PCC is lower than that of one vehicle, whereas in the other three scenarios, the THD_I at the PCC is lower than that of two vehicles. This observation and analysis of the THD_I values provide confidence in the validity of our results and suggest that the cancellation effect of each charging scenario will vary. Since laboratory testing of a high number of EV combinations is not feasible, the next section presents a Monte Carlo simulation to compute the harmonic impacts of a higher number of EVs charging at different rates.

B. MONTE CARLO SIMULATION

To mimic smart charging operations in practice, a Monte Carlo simulation is developed to capture elements of randomness with consideration for different vehicle types and uncertainty in their charging current rates. The output variables acquired through this approach serve as a sample from which the probabilistic distribution of the actual parameters can be estimated. Therefore, confidence in the results increases with the number of simulations. The Monte Carlo simulation has 4 main steps for the specified number of EVs charging simultaneously, which range from 1 to 10:

- *Step 1:* Generate sample input from the EV types and charging current rate.
- *Step 2:* Using vector algebra, compute THD_I by performing vector summation of individual harmonics of the corresponding harmonic content.
- *Step 3:* Repeat Steps 1 & 2 one million times and record THD_I for each iteration.
- *Step 4:* Based on recordings in Step 3, consider all THD_I values and calculate the probability of exceeding harmonic standards. The probability of exceeding harmonic standards is computed by dividing the number of cases (in Step 3) that exceed the harmonic upper limits by the total number of sampling iterations. Mathematically, the probability of failure ($\mathbb{P}_\mathbb{F}$) could be written as

$$\mathbb{P}_\mathbb{F} = \frac{N_F}{N_T}, \tag{3}$$

where N_F is the number of simulation cases that violated the industry limits, and N_T is the total number of simulation cases, which is one million. Calculating (3) requires comparing each simulation case with the industry standard.

Two distinct case studies are implemented as part of the Monte Carlo simulation:

- *Case Study 1* considers EV charging during peak periods and consequently, the charging current is assumed to be between 6A and 10A.
- *Case Study 2* considers off-peak charging and the charging currents are assumed to be higher than 11A.

A critical parameter in Monte Carlo simulations is determining the number of simulation iterations needed to capture the true randomness of the system of interest. To calculate the required number of iterations, the probability of failure for five vehicles charging simultaneously is selected as one of the main indices for harmonic assessment. The number of iterations ranges from 1 to 10 million, and the probability of failure is calculated in Fig. 13. It is evident that the probability reaches its steady state after 10^5 iterations. However, to be on the side of caution, each simulation case is executed for one million iterations for each number of EVs charging, ranging from 1 to 10, to encompass a sufficient range of possible combinations.

There are two primary random inputs for the Monte Carlo simulation. The first one is the vehicle type details, given in Table 3, while the second input is the random charging rate in Amps and associated individual harmonic amplitude and phase angle measured from single EV charging experiments. It is assumed that the vehicle index follows a discrete uniform distribution from 1 to 8, and the probability of choosing a vehicle is equal to $1/8$ at any iteration of the simulation. For Case Study 1, the charging current is randomly selected from a discrete uniform distribution that takes integer values between

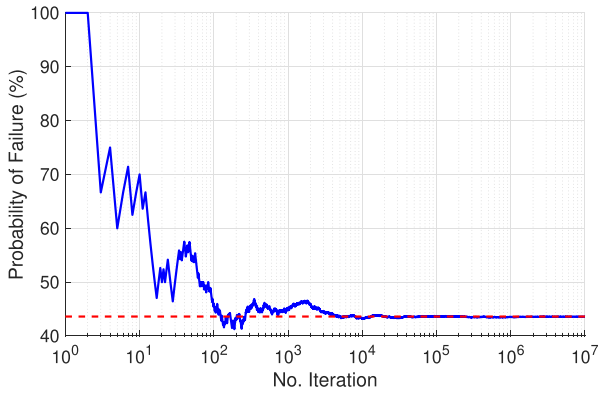

FIGURE 13. Monte Carlo number of iterations decision considering Case Study 1 and 5 EVs charging simultaneously in accordance to 5% THD_I limits.

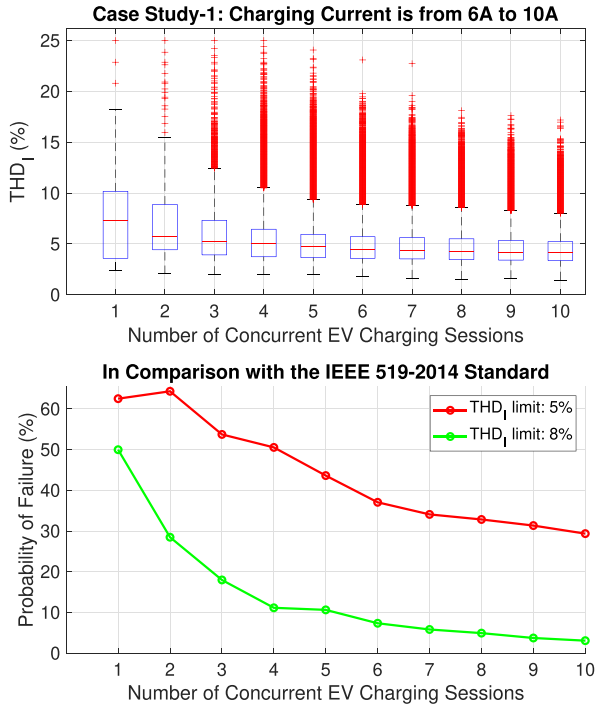

FIGURE 14. Simulation results of multiple simultaneous EV charging for Case Study-1 on THD_I (top) and comparison with IEEE 519-2014 power quality standard (bottom).

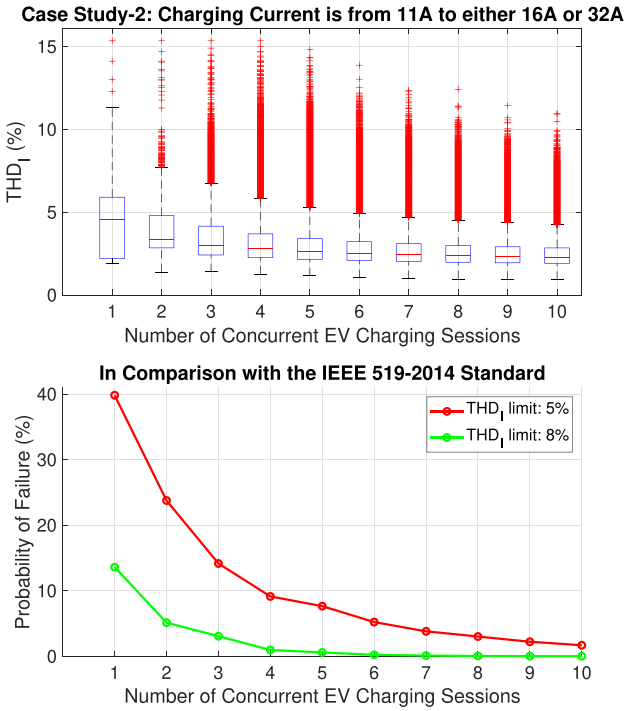

FIGURE 15. Simulation results of multiple simultaneous EV charging for Case Study-2 on THD_I (top) and comparison with IEEE 519-2014 power quality standard (bottom).

6 A and 10 A. Similarly, for Case Study 2, the charging current is randomly chosen from a discrete uniform distribution that takes integer values between 11 A and maximum charging current as given in Table 3.

As a result, THD_I is calculated by vector summation of individual harmonics of the corresponding harmonic content in each iteration. Fig. 14 presents the THD_I for multiple EVs charging simultaneously and the probability of exceeding certain thresholds for 5% and 8%. Each box of THD_I indicates the 25th and 75th percentiles, while the central red mark indicates the median. The whiskers extend to the most extreme data points not considered outliers, and the outliers are plotted individually using the '+' marker symbol. As depicted in Fig. 14, THD_I gradually decreased due to the cancellation effects of harmonic orders. Consequently, the probability of exceeding certain THD_I thresholds has a similar trend.

Moreover, the second Case Study, aiming to mimic off-peak hour charging, is conducted by adjusting the smart charging currents. The results of Case Study 2 are presented in Fig. 15. With increasing charging currents, THD_I decreased by almost half compared to Case Study 1. Consequently, the probability of exceeding the THD_I limits has also decreased significantly. The probability of exceeding the 5% THD_I threshold for charging ten vehicles was approximately 30% in the first case study; this decreased to one-tenth in the second case study. These two case studies demonstrate that while lower smart charging rates are desirable for reducing peak load, the distribution networks will experience power quality issues related to harmonic emissions.

On the other hand, assessing individual harmonics against certain limits set by power quality standards is also crucial. Therefore, Case Study 1 and Case Study 2 are compared with the 5th, 7th, 11th, and 13th harmonics, whose limits are determined by the IEC 61000-3-12 power quality standard. Fig. 16 shows the probabilities of exceeding the specified individual harmonic limits. Since the IEC 61000-3-12 standard considers cases higher than 16A, the number of vehicles charging simultaneously starts with 3 EVs (if 3 EVs are charging with

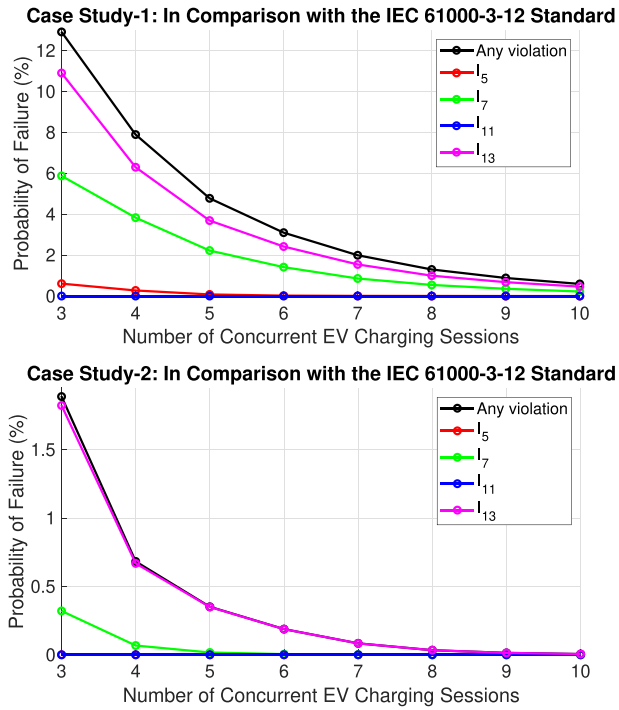

FIGURE 16. Exceeding individual harmonics for two case studies based on IEC 61000-3-12 power quality standard.

6A, the current at the PCC is 18A). One million iterations are conducted for each number of vehicles, and the ratio of the number of iterations with violations to the total number of iterations provides the probability of failure.

In addition to the violation of the 5th, 7th, 11th, and 13th harmonics, which were examined separately, the possibility of exceeding the limit is also considered. Unsurprisingly, the number of individual harmonics exceeding the limits is much higher in Case Study 1. The individual harmonic that exceeds the limits the most is the 13th harmonic. It is seen from Fig. 16 that most individual harmonics that exceed the limits occur at the same time as there is no significant difference between the probability of any individual harmonic violation and the probability of the 13th harmonic violation. Similarly to the THD_I assessment, the probability that Case Study 2 violates the limits is relatively low.

It is noteworthy that this simulation study examines different combinations of EVs and charging rates, thus not representing charging sessions of multiple EVs. A typical charging session could take a couple of hours, during which different charging rates would be assigned to each vehicle. In such cases, charging rates are also limited by the battery state of charge (SoC) levels as the charging current reduces significantly when SoCs are greater than 90%. Nevertheless, the presented results offer critical insights, such as determining vehicle-specific ranges for smart charging.

For instance, the worst-case scenario for multiple EV charging would involve multiple Peugeot e-2008 vehicles charging simultaneously at lower rates. If N of these vehicles are charged simultaneously at 6 Amps, then the THD_I (%) would be around 25%. Conversely, vehicles like the VW ID.4 Pro would not have any vehicle-specific restrictions, as the THD_I levels consistently remain lower than 5%.

VII. CONCLUSIONS AND DISCUSSIONS

This paper provides a detailed analysis of the harmonic emissions associated with the smart charging of electric vehicles (EVs). The study incorporates eight different EV models to represent the diversity of the current market, considering various factors such as age, battery capacity, and on-board charging technologies—both integrated and dedicated. The harmonic emission data collected was analyzed for amplitude, phase angle, and THD, specifically THD_I (current) and THD_V (voltage). The results reveal that vehicles operating at lower smart charging current setpoints experience increased harmonic distortions, leading to higher THD_I levels. Among the vehicles tested, the Peugeot e-2008 displayed the highest THD_I levels, ranging from 11% to 26%, while the Tesla Model Y Long Range and two Renault Zoe models exhibited similar levels of individual harmonic distortions.

The analysis of simultaneous EV charging impacts shows a consistent trend. Both experimental and simulation studies indicate that as more vehicles charge concurrently, THD_I at the PCC slightly decreases. This reduction is due to the phase angle cancellation effect of the harmonics, a phenomenon consistently observed throughout the study. However, despite the overall decrease in THD_I, the first case study focusing on off-peak hour charging revealed that vehicles charging at low power still caused significantly higher harmonic distortion and THD_I.

Power quality standards are crucial for defining the permissible levels of harmonic emissions, which helps ensure the stability and reliability of power grids while minimizing interference and potential damage to connected equipment. The IEC 61000-3-2 standard regulates the allowable harmonic current levels for devices rated up to 16A under conditions that typically produce the highest harmonic content. Meanwhile, IEC 61000-3-12 addresses harmonic limits for devices rated between 16A and 75A. These standards typically evaluate devices in a single operational setting, but smart EV charging introduces dynamic control over charging currents, which can significantly alter the harmonic emission profile, particularly at lower power levels. As a result, smart charging at reduced power can lead to much higher THD_I than operation at rated power. Therefore, there is a need for a new classification system for controllable loads within these standards, with additional harmonic limits defined for different operating points, typically below the rated power. Compliance testing should also be adapted to encompass these multiple operating points.

The findings of this paper underscore the importance of harmonics-aware smart charging strategies that not only support demand-side management but also mitigate harmonic distortion. Furthermore, the study highlights the need for advanced probabilistic models to assess and reduce the harmonic impacts in real-world settings, taking into account both EV

and other non-linear loads connected to the same PCC. These insights lay a strong foundation for future research aimed at refining existing standards to better accommodate the growing integration of EVs into electrical grids.

Moreover, this paper suggests several directions for future research. The scope of this study was limited by the availability of EVs and laboratory resources, which could be expanded in future investigations. First, studying multiple EVs of the same model but of different ages could provide insights into how battery and charger health affect harmonic emissions. Second, exploring the influence of background harmonics, commonly found in residential networks, could shed light on how EV charging harmonics interact with other non-EV loads that exhibit a wide range of characteristics. In addition, the impact of voltage drops on harmonic emissions deserves further investigation. Future studies will use power system simulators such as DigSilent and OpenDSS to explore this relationship, as voltage drops depend on factors like the distance between the PCC and the charger, as well as the influence of other loads sharing the same phase. Simulating such complex networks is essential for accurate analysis.

Additionally, a third research direction will focus on the effects of voltage imbalances caused by EV charging. This is particularly relevant because some EVs charge using single-phase power, while others support three-phase charging. Thus, EV charging could potentially worsen existing power quality issues, including voltage and harmonic imbalances.

REFERENCES

[1] S. Fankhauser et al., "The meaning of net zero and how to get it right," *Nature Climate Change*, vol. 12, no. 1, pp. 15–21, 2022.

[2] W. F. Lamb et al., "A review of trends and drivers of greenhouse gas emissions by sector from 1990 to 2018," *Environ. Res. Lett.*, vol. 16, no. 7, 2021, Art. no. 073005.

[3] European Environment Agency, "Transport and environment report 2021: Decarbonising road transport—The role of vehicles, fuels and transport demand," Pub. Office Eur. Union, Copenhagen, Denmark, Tech. Rep. 02/2022, 2022.

[4] "Can power grids cope with millions of EVs?" Jun. 25, 2024. [Online]. Available: https://tinyurl.com/4pfz626s

[5] K. Sevdari, L. Calearo, P. B. Andersen, and M. Marinelli, "Ancillary services and electric vehicles: An overview from charging clusters and chargers technology perspectives," *Renewable Sustain. Energy Rev.*, vol. 167, 2022, Art. no. 112666.

[6] A. Opstad, B. H. Bekken, H. S. Nygård, G. Doorman, and K. Sevdari, "Flexibility from electric vehicles-residential charging coincidence factors in Norway," in *Proc. CIGRE Paris Session 2024*, 2024.

[7] M. H. Tveit, K. Sevdari, M. Marinelli, and L. Calearo, "Behind-the-meter residential electric vehicle smart charging strategies: Danish cases," in *Proc. Int. Conf. Renewable Energies Smart Technol.*, 2022, pp. 1–5.

[8] T. Zeng, H. Zhang, and S. Moura, "Solving overstay and stochasticity in PEV charging station planning with real data," *IEEE Trans. Ind. Inform.*, vol. 16, no. 5, pp. 3504–3514, May 2020.

[9] I. S. Bayram, A. Saad, R. Sims, A. Babu, C. Edmunds, and S. Galloway, "Statistical characterisation of public AC EV chargers in the U.K.," *IEEE Access*, vol. 11, pp. 70274–70287, 2023.

[10] L. Calearo, M. Marinelli, and C. Ziras, "A review of data sources for electric vehicle integration studies," *Renewable Sustain. Energy Rev.*, vol. 151, 2021, Art. no. 111518.

[11] S. Striani, K. Sevdari, P. B. Andersen, M. Marinelli, Y. Kobayashi, and K. Suzuki, "Autonomously distributed control of EV parking lot management for optimal grid integration," in *Proc. IEEE Int. Conf. Renewable Energies Smart Technol.*, 2022, pp. 1–5.

[12] U.K. Government Electric Vehicle Smart Charging. Jun. 25, 2024. [Online]. Available: https://tinyurl.com/36p96eu9

[13] "Largest smart electric vehicle charging network optimises use of renewable energy in amsterdam," Sep. 2024. [Online]. Available: https://tinyurl.com/37y3azr3

[14] A. Dubey and S. Santoso, "Electric vehicle charging on residential distribution systems: Impacts and mitigations," *IEEE Access*, vol. 3, pp. 1871–1893, 2015.

[15] C. McGarry et al., "Electrified heat and transport: Energy demand futures, their impacts on power networks and what it means for system flexibility," *Appl. Energy*, vol. 360, 2024, Art. no. 122836.

[16] Z. J. Lee et al., "Adaptive charging networks: A framework for smart electric vehicle charging," *IEEE Trans. Smart Grid*, vol. 12, no. 5, pp. 4339–4350, Sep. 2021.

[17] G. Barone et al., "How smart metering and smart charging may help a local energy community in collective self-consumption in presence of electric vehicles," *Energies*, vol. 13, no. 16, 2020, Art. no. 4163.

[18] A. Khaligh and M. D'Antonio, "Global trends in high-power on-board chargers for electric vehicles," *IEEE Trans. Veh. Technol.*, vol. 68, no. 4, pp. 3306–3324, Apr. 2019.

[19] S. Taghizadeh, M. Hossain, J. Lu, and W. Water, "A unified multi-functional on-board EV charger for power-quality control in household networks," *Appl. Energy*, vol. 215, pp. 186–201, 2018.

[20] K. Sevdari, L. Calearo, B. H. Bakken, P. B. Andersen, and M. Marinelli, "Experimental validation of onboard electric vehicle chargers to improve the efficiency of smart charging operation," *Sustain. Energy Technol. Assessments*, vol. 60, 2023, Art. no. 103512.

[21] D. Alame, M. Azzouz, and N. Kar, "Assessing and mitigating impacts of electric vehicle harmonic currents on distribution systems," *Energies*, vol. 13, no. 12, 2020, Art. no. 3257.

[22] A. Ulinuha and E. M. Sari, "The influence of harmonic distortion on losses and efficiency of three-phase distribution transformer," in *J. Physics: Conf. Ser.*, vol. 1858, no. 1. 2021, Art. no. 012084.

[23] J. Yuan, L. Dorn-Gomba, A. D. Callegaro, J. Reimers, and A. Emadi, "A review of bidirectional on-board chargers for electric vehicles," *IEEE Access*, vol. 9, pp. 51501–51518, 2021.

[24] R. Pinyol, "Harmonics: Causes, effects and minimization," Salicru White Papers, pp. 1–32, 2015.

[25] T. Slangen, T. van Wijk, V. Ćuk, and J. Cobben, "The harmonic and supraharmonic emission of battery electric vehicles in The Netherlands," in *Proc. IEEE Int. Conf. Smart Energy Syst. Technol.*, 2020, pp. 1–6.

[26] I. S. Bayram and A. Tajer, *Plug-In Electric Vehicle Grid Integration*. Norwood, MA, USA: Artech House, 2017.

[27] S. Striani, K. Sevdari, L. Calearo, P. B. Andersen, and M. Marinelli, "Barriers and solutions for EVs integration in the distribution grid," in *Proc. IEEE 56th Int. Universities Power Eng. Conf.*, 2021, pp. 1–6.

[28] E. Karabiyik and A. S. Karabiyik, "Investigation of long short-term memory networks in short-term electric vehicle charging load modeling," in *Proc. IEEE 14th Int. Conf. Elect. Electron. Eng.*, 2023, pp. 1–5.

[29] H. S. Das, M. M. Rahman, S. Li, and C. W. Tan, "Electric vehicles standards, charging infrastructure, and impact on grid integration: A technological review," *Renewable Sustain. Energy Rev.*, vol. 120, 2020, Art. no. 109618.

[30] L. Calearo, A. Thingvad, K. Suzuki, and M. Marinelli, "Grid loading due to EV charging profiles based on pseudo-real driving pattern and user behavior," *IEEE Trans. Transport. Electrific.*, vol. 5, no. 3, pp. 683–694, Sep. 2019.

[31] D. Luca de Tena and T. Pregger, "Impact of electric vehicles on a future renewable energy-based power system in Europe with a focus on Germany," *Int. J. Energy Res.*, vol. 42, no. 8, pp. 2670–2685, 2018.

[32] I. Koncar and I. S. Bayram, "A probabilistic methodology to quantify the impacts of cold weather on electric vehicle demand: A case study in the u.k," *IEEE Access*, vol. 9, pp. 88205–88216, 2021.

[33] M. Senol, I. S. Bayram, Y. Naderi, and S. Galloway, "Electric vehicles under low temperatures: A. review on battery performance, charging needs, and power grid impacts," *IEEE Access*, vol. 11, pp. 39879–39912, 2023.

[34] Y. Li and A. Jenn, "Impact of electric vehicle charging demand on power distribution grid congestion," *Proc. Nat. Acad. Sci.*, vol. 121, no. 18, 2024, Art. no. e2317599121.

[35] M. Soleimani and M. Kezunovic, "Mitigating transformer loss of life and reducing the hazard of failure by the smart EV charging," *IEEE Trans. Ind. Appl.*, vol. 56, no. 5, pp. 5974–5983, Sep./Oct. 2020.

[36] R. Pogaki, "Western power distribution electric vehicle charging (PSE0564001)," Tech. Rep. PSE0564001-H1 Rev. 21, 2018.

[37] N. Zhou, J. Wang, Q. Wang, and N. Wei, "Measurement-based harmonic modeling of an electric vehicle charging station using a three-phase uncontrolled rectifier," *IEEE Trans. Smart Grid*, vol. 6, no. 3, pp. 1332–1340, May 2015.

[38] G. Foskolos, "Measurement-based current-harmonics modeling of aggregated electric-vehicle loads using power-exponential functions," *World Electric Veh. J.*, vol. 11, no. 3, 2020, Art. no. 51.

[39] J. Gomez and M. Morcos, "Impact of EV battery chargers on the power quality of distribution systems," *IEEE Trans. Power Del.*, vol. 18, no. 3, pp. 975–981, Jul. 2003.

[40] A. K. Karmaker, S. Roy, and M. R. Ahmed, "Analysis of the impact of electric vehicle charging station on power quality issues," in *Proc. 2019 IEEE Int. Conf. Elect., Computer Commun. Eng.*, 2019, pp. 1–6.

[41] D. Contreras Ramírez and L.-G. Juan, "K-Factor analysis to increase the actual capacity of electrical distribution transformers," in *Commun.,Smart Technol. Innov. Soc., Proc. CITIS 2021*. Springer, 2022, pp. 367–379.

[42] IEEE Std C57.91-2011, *IEEE Guide for Loading Mineral-Oil-Immersed Transformers and Step-Voltage Regulators*, Institute of Electrical and Electronics Engineers (IEEE), Standard, 2012.

[43] N. R. Kalaskar and R. Holmukhe, "Report on power compensation and total harmonic distortion level analysis," *Int. J. Elect. Comput. Eng.*, vol. 6, no. 6, 2016, Art. no. 2577.

[44] P. Mazurek and A. Chudy, "An analysis of electromagnetic disturbances from an electric vehicle charging station," *Energies*, vol. 15, no. 1, 2021, Art. no. 244.

[45] S. S. G. Acharige, M. E. Haque, M. T. Arif, N. Hosseinzadeh, K. N. Hasan, and A. M. T. Oo, "Review of electric vehicle charging technologies, standards, architectures, and converter configurations," *IEEE Access*, vol. 11, pp. 41218–41255, 2023.

[46] A. Lucas, F. Bonavitacola, E. Kotsakis, and G. Fulli, "Grid harmonic impact of multiple electric vehicle fast charging," *Electric Power Syst. Res.*, vol. 127, pp. 13–21, 2015.

[47] A. Collin et al., "Survey of harmonic emission of electrical vehicle chargers in the European market," in *Proc. IEEE Int. Symp. Power Electronics, Elect. Drives, Automat. Motion*., 2016, pp. 1208–1213.

[48] S. Gugliotta, "Interaction between current harmonics produced by different electric vehicles DC chargers," Ph.D. dissertation, Politecnico di Torino, 2024.

[49] IEEE 519-2014, *IEEE Recommended Practice and Requirements for Harmonic Control in Electric Power Systems*, Institute of Electrical and Electronics Engineers (IEEE), Standard, 2014.

[50] I. Ziyat, A. Gola, P. R. Palmer, S. Makonin, and F. Popowich, "EV charging profiles and waveforms dataset (EV-CPW) and associated power quality analysis," *IEEE Access*, vol. 11, pp. 138445–138456, 2023.

[51] S. M. Miraftabzadeh, D. Pejovski, M. Longo, M. Brenna, and M. Pasetti, "Impact of electric vehicle charging on voltage and current harmonics at the point of common coupling," in *Proc. IEEE Int. Conf. Environ. Elect. Eng. Ind. Commercial Power Syst. Eur.*, 2023, pp. 1–6.

[52] G. Ye, V. Cuk, and J. F. Cobben, "A study on harmonic current summation using field measurement data," in *Proc. IEEE Int. Conf. Power System Technol.*, 2016, pp. 1–6.

[53] IEC TR 61000-3-6, "Electromagnetic compatibility (EMC)–Part 3-6: Limits–Assessment of emission limits for the connection of distorting installations to MV, HV and EHV power systems," International Electrotechnical Commission (IEC), Tech. Rep. 61000-3-6, 2008.

[54] J. Wikston, "Harmonic summation for multiple arc furnaces," in *Proc. IEEE Power Eng. Soc. Winter Meeting. Conf. Proc.*, 2002, pp. 1072–1075.

[55] S. Xie, Q. Li, L. Zhao, and Y. Xu, "Study on summation exponents of harmonic of electrified railway," in *Proc. IEEE 5th Int. Conf. Power Electron. Drive Syst.*, 2003. PEDS, 2003, pp. 816–820.

[56] F. Medeiros, D. C. Brasil, C. A. Marques, C. A. Duque, and P. F. Ribeiro, "Considerations on the aggregation of harmonics produced by large wind farms," in *Proc. IEEE 15th Int. Conf. Harmon. Qual. Power.*, 2012, pp. 364–369.

[57] K. Daniel et al., "Current harmonic aggregation cases for contemporary loads," *Energies*, vol. 15, no. 2, 2022, Art. no. 437.

[58] L. Kütt, E. Saarijärvi, M. Lehtonen, H. Molder, and J. Niitsoo, "Estimating the harmonic distortions in a distribution network supplying EV charging load using practical source data—Case example," in *Proc. IEEE PES Gen. Meeting | Conf. & Expo.*, 2014, pp. 1–5.

[59] IEC 61000-3-2, *Electromagnetic Compatibility (EMC) - Part 3-2: Limits - Limits for Harmonic Current Emissions (Equipment Input Current ≤ 16 A Per Phase)*," International Electrotechnical Commission (IEC), Standard, 2018.

[60] IEC 61000-3-12, *Electromagnetic Compatibility (EMC) - Part 3-12: Limits - Limits for Harmonic Currents produced by Equipment Connected to Public Low-voltage Systems with Input Current* > 16 *A. and ≤ 75 A. per Phase*, International Electrotechnical Commission (IEC), Standard, 2021.

[61] IEC 61000-2-2, *Electromagnetic compatibility (EMC) - Part 2-2: Environment - Compatibility Levels for Low-Frequency Conducted Disturbances and Signalling in Public Low-voltage Power Supply Systems*, International Electrotechnical Commission (IEC), Standard, 2002.

[62] IEC 61000-2-4, *Electromagnetic compatibility (EMC) - Part 2-4: Environment - Compatibility Levels in Industrial Plants for Low-frequency Conducted Disturbances*, International Electrotechnical Commission (IEC), Standard, 2002.

[63] IEC 61000-4-7, *Electromagnetic compatibility (EMC) - Part 4-7: Testing and Measurement Techniques - General Guide on Harmonics and Interharmonics Measurements and Instrumentation, for Power Supply Systems and Equipment Connected Thereto*, International Electrotechnical Commission (IEC), Standard, 2002.

[64] IEC 61000-4-30, *Electromagnetic Compatibility (EMC) - Part 4-30: Testing and Measurement Techniques - Power Quality Measurement Methods*, International Electrotechnical Commission (IEC), Standard, 2015.

[65] EN 50160, *CENELEC - EN 50160: Voltage Characteristics of Electricity Supplied by Public Distribution Systems*, European Committee for Electrotechnical Standardization (CENELEC), Standard, 2010.

[66] Energy System Integration Lab - SYSLAB. Jun. 2024. [Online]. Available: https://tinyurl.com/3cy6r8vt

[67] "Measurement-based harmonic analysis of electric vehicle smart charging," Univ. Strathclyde, Nov. 2024. [Online]. Available: https://pureportal.strath.ac.uk/en/datasets/data-for-measurement-based-harmonic-analysis-of-electric-vehicle-

[68] K. Sevdari, "Control and clustering of electric vehicle chargers for the provision of grid services," Ph.D. dissertation, Technical University of Denmark, 2023.

[69] Fronius Wattpilot AC Smart Charger. Jun. 2024. [Online]. Available: https://tinyurl.com/4xp4rew3

[70] Zaptec Pro AC Smart Charger. Jun. 25, 2024. [Online]. Available: https://tinyurl.com/4uebhdvv

[71] KeContact P30 X-series AC smart charger. Jun. 25, 2024. [Online]. Available: https://tinyurl.com/4jkpntmx

[72] Yokogawa WT500 mid-range power analyzer. Jun. 25, 2024. [Online]. Available: https://tinyurl.com/3k896hkp

[73] Users manual for fluke 434-II/435-II/437-II. Jun. 25, 2024. [Online]. Available: https://tinyurl.com/3*p58nu59*.

[74] IEC 61851-1, *Electric Vehicle Conductive Charging System-Part 1, General Requirements*, International Electrotechnical Commission (IEC), Standard, 2017.

[75] D. Shmilovitz, "On the definition of total harmonic distortion and its effect on measurement interpretation," *IEEE Trans. Power Del.*, vol. 20, no. 1, pp. 526–528, Jan. 2005.

[76] A. G. Asuero, A. Sayago, and A. González, "The correlation coefficient: An overview," *Crit. Rev. Anal. Chem.*, vol. 36, no. 1, pp. 41–59, 2006.

[77] P. Berens, "CircStat: A. MATLAB toolbox for circular statistics," *J. Stat. Softw.*, vol. 31, no. 10, pp. 1–21, 2009. [Online]. Available: https://tinyurl.com/ycxjj8aw

[78] L. M. A. Alsaqal, A. M. I. Alnaib, and O. T. Mahmood, "Comparison of multiple modulation techniques for various topologies of multilevel converters for single phase AC motor drive," *Int. J. Power Electron. Drive Syst.*, vol. 2088, no. 8694, 2019, Art. no. 8694.

[79] V. Ćuk, J. F. Cobben, W. L. Kling, and P. F. Ribeiro, "Analysis of harmonic current summation based on field measurements," *IET Gener., Transmiss. Distrib.*, vol. 7, no. 12, pp. 1391–1400, 2013.